

# The Ligo-Ligo cross correlation for the detection of relic scalar gravitational waves

Christian Corda

February 14, 2021

International Institute for Theoretical Physics and Advanced Mathematics  
Einstein-Galilei, Via Santa Gonda, 14 - 59100 Prato, Italy

*E-mail address:* [cordac.galilei@gmail.com](mailto:cordac.galilei@gmail.com)

## Abstract

In the earlier work arXiv:0706.3782 we studied the cross correlation between the Virgo interferometer and the MiniGRAIL resonant sphere for the detection of relic scalar gravitational waves (SGWs). We have shown that the overlap reduction function for the cross correlation between Virgo and the monopole mode of MiniGRAIL is very small, but a maximum was also found in the correlation at about  $2710\text{Hz}$ , in the range of the MiniGRAIL sensitivity.

In this paper the analysis is improved. After carefully reviewing the response function of interferometers to SGWs directly in the gauge of the local observer, the result is used to analyze the cross correlation between the two LIGO interferometers in their advanced configuration for a potential detection of relic SGWs and to release a lower bound for the integration time of such a detection. By using a new, frequency-dependent, overlap reduction function, a comparison with previous low-frequency approximations is therefore discussed.

This is the first time that such a cross-correlation is computed in all the frequency spectrum of relic SGWs. The computation of a better signal to noise ratio is very important to understand if a scalar component of GWs is present at high frequency. With the new overlap reduction function, an order of magnitude is gained concerning the integration time for detecting the relic SGWs' signal. This could be very important for a potential detection if advanced projects further improve their sensitivity.

PACS numbers: 04.80.Nn, 04.30.Nk, 04.50.+h

# 1 Introduction

One of the most important goals of interferometric GWs detectors (for the current status of GWs interferometers see [1]) is the detection of relic GWs that would carry, if detected, a huge amount of information on the early stages of the Universe evolution (see the recent review [2], the recent results [3]-[7] and references within).

The mechanism of production of relic GWs is well known. The quantum fluctuations in the spacetime geometry during the inflationary era generated relic GWs which would have imprinted tensor perturbations on the Cosmic Microwave Background Radiation anisotropy. The GWs perturbations arise from the uncertainty principle and the spectrum of relic GWs is generated from the adiabatically-amplified zero-point fluctuations [2]-[7]. The detection of relic GWs is the only way to learn about the evolution of the very early universe, up to the bounds of the Planck epoch and the initial singularity [2]-[7]. The potential production of relic GWs has been extended in the framework of scalar-tensor theories of gravity in [8].

In earlier work we studied the cross correlation between the Virgo interferometer and the MiniGRAIL resonant sphere for the detection of relic SGWs [9]. In such a work we have shown that the overlap reduction function for the cross correlation between Virgo and the monopole mode of MiniGRAIL is very small, but a maximum was also found in the correlation at about 2710Hz, in the range of the MiniGRAIL sensitivity.

In this paper the analysis is improved. After carefully reviewing the response function of interferometers to SGWs directly in the gauge of the local observer, the result is used to analyze the cross correlation between the two LIGO interferometers in their advanced configuration for a potential detection of relic SGWs and to release a lower bound for the integration time of such a detection. In this way, by using a new, frequency-dependent, overlap reduction function, a comparison with previous low-frequency approximations is realized. Note that this is the first time that such a cross correlation is computed in all the frequency spectrum of relic SGWs. Then, our computation of a better signal to noise ratio is very important to understand if a scalar component of GWs could be present at high frequency.

More, with the new overlap reduction function, an order of magnitude is gained concerning the integration time for detecting the signal from relic SGWs. This could be very important for a potential detection if advanced projects further improve their sensitivity.

It is important to mention the observational constraints to relic SGWs. Such relic SGWs can be analyzed in terms of the scalar field  $\Phi$  and characterized by a dimensionless spectrum [8] (notice that in this paper natural units are used:  $G = 1$ ,  $c = 1$  and  $\hbar = 1$ ):

$$\Omega_{sgw}(f) = \frac{1}{\rho_c} \frac{d\rho_{sgw}}{d \ln f}, \quad (1)$$

where

$$\rho_c \equiv \frac{3H_0^2}{8G} \quad (2)$$

is the (actual) critical density energy of the Universe [13].

Concerning an inflationary flat spectrum, recent computations released the bound [8, 14]

$$\Omega_{sgw}(f)h_{100}^2 < 10^{-13}. \quad (3)$$

The cross correlation between the two LIGO interferometers which is computed in the present work is fundamental for the high-frequency portion of the spectrum (3) that falls in the frequency-range of Earth based interferometers. Such a frequency-range is the interval [1]

$$10Hz \leq f \leq 1KHz. \quad (4)$$

Previous cross-correlations, like the one in [12], only covered the shorter low-frequencies portion

$$10Hz \leq f \leq 100Hz. \quad (5)$$

In fact, earlier overlap reduction functions were constructed with approximated low-frequency response functions which did not cover the high-frequency portion of the interval  $100Hz \leq f \leq 1KHz$ .

## 2 A review of the frequency-dependent response function

The frequency-dependent response function for SGWs has been carefully computed in [9, 10] where previous computations in the low frequency approximation [11, 12] have been generalized.

As detectors of GW work in a laboratory environment on Earth [1, 10], it is quite important to compute the response function in the gauge of the local observer [1]. In this review section we retrieve the same results of [9, 10], where the computation was realized in the transverse-traceless (TT) gauge.

In the gauge of the local observer, SGWs manifest themselves by exerting tidal forces on the masses (the mirror and the beam-splitter in the case of an interferometer). In this gauge the time coordinate  $x_0$  is the proper time of the observer O, spatial axes are centered in O and in the special case of zero acceleration and zero rotation the spatial coordinates  $x_j$  are the proper distances along the axes and the frame of the local observer reduces to a local Lorentz frame [16]. In that case the line element reads [16]

$$ds^2 = -(dx^0)^2 + \delta_{ij}dx^i dx^j + O(|x^j|^2)dx^\alpha dx^\beta, \quad (6)$$

and the effect of GWs on test masses is described by the equation for geodesic deviation [16]

$$\ddot{x}^i = -\tilde{R}_{0k0}^i x^k, \quad (7)$$

where  $\tilde{R}_{0k0}^i$  are the components of the linearized Riemann tensor.

By following [9, 10, 18], a good way to analyze variations in the proper distance (time) is by means of “bouncing photons”. A photon can be launched from the interferometer’s beam-splitter to be bounced back by the mirror. In the gauge of the local observer, two different effects have to be considered in the calculation of the variation of the round-trip time for photons. The variations of the coordinates of the mirror of the interferometer in presence of a SGW, in the frame of the local observer are [10]

$$\delta x(t) = \frac{1}{2}x_0\Phi(t) \quad (8)$$

and

$$\delta y(t) = \frac{1}{2}y_0\Phi(t). \quad (9)$$

$\Phi(t + z)$  is the amplitude of the SGW,  $x_0$  and  $y_0$  are the the unperturbed values of the variables, see [10] for details. Eqs. (8) and (9) have been obtained by using the perturbation method [16] from the equation of motion which are [10]

$$\ddot{x} = \frac{1}{2}\ddot{\Phi}x \quad (10)$$

and

$$\ddot{y} = \frac{1}{2}\ddot{\Phi}y. \quad (11)$$

To compute the response function for an arbitrary propagating direction of the SGW one recalls that the arms of the interferometer are in the  $\vec{u}$  and  $\vec{v}$  directions, while the  $x, y, z$  frame is adapted to the propagating SGW. Then, a spatial rotation of the coordinate system has to be realized

$$\begin{aligned} u &= -x \cos \theta \cos \phi + y \sin \theta \cos \phi \\ v &= -x \cos \theta \sin \phi - y \cos \theta \sin \phi + z \sin \theta \sin \phi \\ w &= x \sin \theta + z \cos \theta, \end{aligned} \quad (12)$$

or, in terms of the  $x, y, z$  frame

$$\begin{aligned} x &= -u \cos \theta \cos \phi - v \cos \theta \sin \phi + w \sin \theta \\ y &= u \sin \theta \cos \phi - v \sin \theta \sin \phi \\ z &= u \sin \theta \sin \phi + v \sin \theta \cos \phi + w \cos \theta. \end{aligned} \quad (13)$$

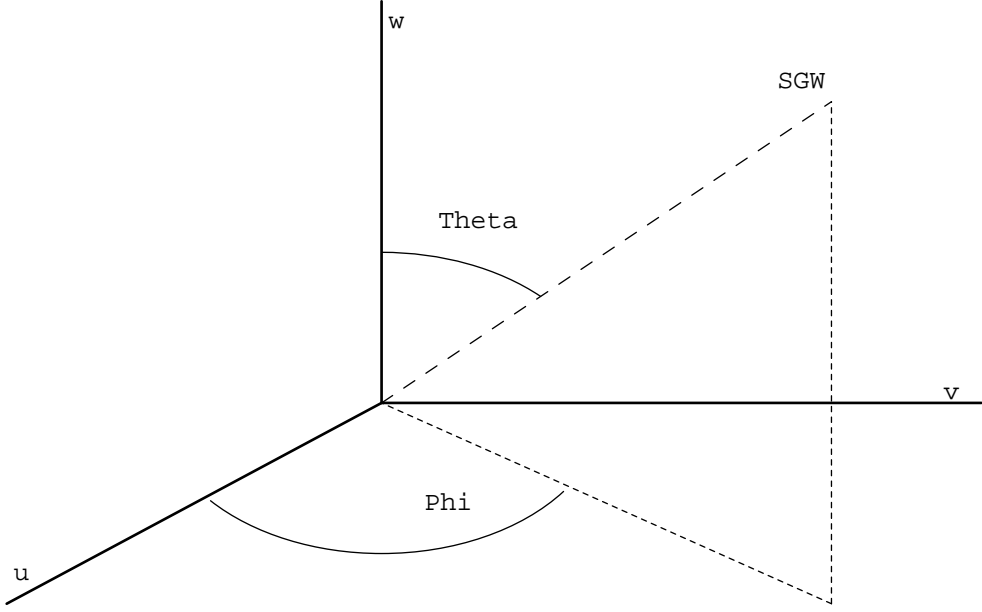


Figure 1: a SGW propagating from an arbitrary direction, adapted from ref. [10]

In this way, the SGW is propagating from an arbitrary direction  $\vec{r}$  to the interferometer (see figure 1). By assuming that the mirror of eqs. (8) and (9) is located in the  $u$  direction, if one uses eqs. (12), (13), (8) and (9), the  $u$  coordinate of the mirror is

$$u = L + \frac{1}{2}LA\Phi(t - u \sin \theta \cos \phi), \quad (14)$$

where

$$A \equiv \cos^2 \theta \cos^2 \phi + \sin^2 \phi. \quad (15)$$

We start with a photon which propagates in the  $u$  axis. The analysis is almost the same for a photon which propagates in the  $v$  axis. By putting the origin of the coordinate system in the beam splitter of the interferometer and using eq. (14), the unperturbed coordinates of the beam-splitter and of the mirror are  $u_b = 0$  and  $u_m = L$ . The unperturbed propagation time between the two masses is

$$T = L. \quad (16)$$

From eq. (14) the displacements of the two masses under the influence of the SGW are

$$\delta u_b(t) = 0 \quad (17)$$

and

$$\delta u_m(t) = \frac{1}{2}LA\Phi(t - L \sin \theta \cos \phi). \quad (18)$$

The relative displacement, which is defined by

$$\delta L(t) = \delta u_m(t) - \delta u_b(t), \quad (19)$$

gives

$$\frac{\delta T(t)}{T} = \frac{\delta L(t)}{L} = \frac{1}{2}LA\Phi(t - L \sin \theta \cos \phi). \quad (20)$$

But, for a large separation between the test masses (in the case of Virgo the distance between the beam-splitter and the mirror is three kilometers, four in the case of LIGO), the definition (19) for relative displacements is not physically viable because the two test masses are taken at the same time and therefore cannot be in a causal connection [10]. The correct definitions for the bouncing photon are

$$\delta L_1(t) = \delta u_m(t) - \delta u_b(t - T_1) \quad (21)$$

and

$$\delta L_2(t) = \delta u_m(t - T_2) - \delta u_b(t), \quad (22)$$

where  $T_1$  and  $T_2$  are the photon propagation times for the forward and return trip correspondingly.  $t$  is the time at which the photon completes its travel down the arm [19]. Thus, in (21),  $t$  is the time that the photon strikes the mirror [19]. In (22),  $t$  is the time that the photon strikes the beam splitter [19]. According to the new definitions, the displacement of one test mass is compared with the displacement of the other at a later time in order to allow a finite delay for the light propagation [10]. The propagation times  $T_1$  and  $T_2$  in eqs. (21) and (22) can be replaced with the nominal value  $T$  because the test mass displacements are already first order in  $\Phi$  [10]. The total change in the distance between the beam splitter and the mirror, in one round-trip of the photon, is

$$\delta L_{r.t.}(t) = \delta L_1(t - T) + \delta L_2(t) = 2\delta u_m(t - T) - \delta u_b(t) - \delta u_b(t - 2T), \quad (23)$$

and in terms of the amplitude of the SGW

$$\delta L_{r.t.}(t) = LA\Phi(t - L \sin \theta \cos \phi - L). \quad (24)$$

In eqs. (23) and (24)  $t$  is the time that the photon strikes the beam splitter [19]. The change in distance (24) leads to changes in the round-trip time for photons propagating between the beam-splitter and the mirror

$$\frac{\delta_1 T(t)}{T} = A\Phi(t - L \sin \theta \cos \phi - L). \quad (25)$$

In the last calculation (variations in the photon round-trip time which come from the motion of the test masses induced by the SGW), we implicitly assumed that the propagation of the photon between the beam-splitter and the mirror of the interferometer is uniform as if it moved in a flat space-time. But, the presence of the tidal forces indicates that the space-time is curved [16]. As a result one more effect after the first discussed has to be considered, which requires spacial separation [10].

From eqs. (10), (11), (12) and (13) the tidal acceleration of a test mass caused by the SGW in the  $u$  direction is

$$\ddot{u}(t - u \sin \theta \cos \phi) = \frac{1}{2} LA \ddot{\Phi}(t - u \sin \theta \cos \phi). \quad (26)$$

Equivalently one can say that there is a gravitational potential [10, 16]

$$V(u, t) = -\frac{1}{2} LA \int_0^u \ddot{\Phi}(t - l \sin \theta \cos \phi) dl, \quad (27)$$

which generates the tidal forces, and that the motion of the test mass is governed by the Newtonian equation

$$\ddot{\vec{r}} = -\bigtriangledown V. \quad (28)$$

For the second effect, the interval for photons propagating along the  $u$  - axis can be written like

$$ds^2 = g_{00} dt^2 - du^2. \quad (29)$$

The condition for a null trajectory  $ds = 0$  gives the coordinate velocity of the photons

$$v_p^2 \equiv \left(\frac{du}{dt}\right)^2 = 1 + 2V(t, u), \quad (30)$$

which, to first order in  $\Phi$ , is approximated by

$$v_p \approx \pm[1 + V(t, u)], \quad (31)$$

with  $+$  and  $-$  for the forward and return trip respectively. By knowing the coordinate velocity of the photon, the propagation time for its traveling between the beam-splitter and the mirror can be defined:

$$T_1(t) = \int_{u_b(t-T_1)}^{u_m(t)} \frac{du}{v_p} \quad (32)$$

and

$$T_2(t) = \int_{u_m(t-T_2)}^{u_b(t)} \frac{(-du)}{v_p}. \quad (33)$$

The calculations of these integrals would be complicated because the  $u_m$  boundaries of them are changing with time [10]

$$u_b(t) = 0 \quad (34)$$

and

$$u_m(t) = L + \delta u_m(t). \quad (35)$$

But, to first order in  $\Phi$ , these contributions can be approximated by  $\delta L_1(t)$  and  $\delta L_2(t)$  (see eqs. (21) and (22)). The combined effect of the varying boundaries is given by  $\delta_1 T(t)$  in eq. (25) and only the times for photon propagation between the fixed boundaries 0 and  $L$  have to be computed [10]. Such propagation times will be indicated with  $\Delta T_{1,2}$  to distinguish from  $T_{1,2}$ . In the forward trip, the propagation time between the fixed limits is

$$\Delta T_1(t) = \int_0^L \frac{du}{v_p(t', u)} \approx L - \int_0^L V(t', u) du, \quad (36)$$

where  $t'$  is the delay time (i.e.  $t$  is the time at which the photon arrives in the position  $L$ , so  $L - u = t - t'$ ) which corresponds to the unperturbed photon trajectory:

$$t' = t - (L - u).$$

Similarly, the propagation time in the return trip is

$$\Delta T_2(t) = L - \int_L^0 V(t', u) du, \quad (37)$$

where now the delay time is given by

$$t' = t - u.$$

The sum of  $\Delta T_1(t - T)$  and  $\Delta T_2(t)$  gives the round-trip time for photons traveling between the fixed boundaries. The deviation of this round-trip time (distance) from its unperturbed value  $2T$  is

$$\begin{aligned} \delta_2 T(t) = & - \int_0^L [V(t - 2L + u, u) du + \\ & - \int_L^0 V(t - u, u) du], \end{aligned} \quad (38)$$

and, by using eq. (27),

$$\begin{aligned} \delta_2 T(t) = & \frac{1}{2} LA \int_0^L [\int_0^u \ddot{\Phi}(t - 2T + l(1 - \sin \theta \cos \phi)) dl + \\ & - \int_0^u \ddot{\Phi}(t - l(1 + \sin \theta \cos \phi)) dl] du. \end{aligned} \quad (39)$$

The total round-trip proper time in presence of the SGW is

$$T_t = 2T + \delta_1 T + \delta_2 T, \quad (40)$$

and

$$\delta T_u = T_t - 2T = \delta_1 T + \delta_2 T \quad (41)$$

is the total variation of the proper time for the round-trip of the photon in presence of the SGW in the  $u$  direction.

By using eqs. (25), (39) and the Fourier transform of  $\Phi$  defined by

$$\tilde{\Phi}(\omega) = \int_{-\infty}^{\infty} dt \Phi(t) \exp(i\omega t), \quad (42)$$

the quantity (41) can be computed in the frequency domain [10] as

$$\tilde{\delta}T_u(\omega) = \tilde{\delta}_1 T(\omega) + \tilde{\delta}_2 T(\omega) \quad (43)$$

where

$$\tilde{\delta}_1 T(\omega) = \exp[i\omega L(1 + \sin \theta \cos \phi)] L A \tilde{\Phi}(\omega) \quad (44)$$

$$\begin{aligned} \tilde{\delta}_2 T(\omega) = & -\frac{LA}{2} \left[ \frac{-1 + \exp[i\omega L(1 + \sin \theta \cos \phi)] - iL\omega(1 + \sin \theta \cos \phi)}{(1 + \sin \theta \cos \phi)^2} + \right. \\ & \left. + \frac{\exp(2i\omega L)(1 - \exp[i\omega L(-1 + \sin \theta \cos \phi)] + iL\omega - (1 + \sin \theta \cos \phi)}{(-1 + \sin \theta \cos \phi)^2} \right] \tilde{\Phi}(\omega). \end{aligned} \quad (45)$$

In the above computation, the derivative and translation theorems on the Fourier transform have been used. By using eq. (15), the response function of the  $u$  arm of the interferometer to the SGW is obtained

$$\begin{aligned} H_u(\omega) = & \frac{\tilde{\delta}T_u(\omega)}{L\tilde{\Phi}(\omega)} = \frac{1}{2i\omega L} [-1 + \exp(2i\omega L) + \\ & + \sin \theta \cos \phi ((1 + \exp(2i\omega L) - 2 \exp i\omega L(1 + \sin \theta \cos \phi))]. \end{aligned} \quad (46)$$

Eq. (46) is the same result of equation (148) in [10], where the computation has been realized in TT gauge.

The computation for the  $v$  arm is similar to the one above. We do not write down redundant computations and we give the direct result

$$\begin{aligned} H_v(\omega) = & \frac{\tilde{\delta}T_u(\omega)}{L\tilde{\Phi}(\omega)} = \frac{1}{2i\omega L} [-1 + \exp(2i\omega L) + \\ & + \sin \theta \sin \phi ((1 + \exp(2i\omega L) - 2 \exp i\omega L(1 + \sin \theta \sin \phi))], \end{aligned} \quad (47)$$

which is exactly the result (149) in [10], where the computation has been made in the TT gauge.

The total response function is given by the difference of the two response functions of the two arms [1, 9, 10]

$$H_{tot}(\omega) = H_u(\omega) - H_v(\omega), \quad (48)$$

and, by using eqs. (46) and (47), one gets

$$H_{tot}(\omega) = \frac{\delta T_{tot}(\omega)}{L\Phi(\omega)} = \frac{\sin \theta}{2i\omega L} \{ \cos \phi [1 + \exp(2i\omega L) - 2 \exp i\omega L (1 + \sin \theta \cos \phi)] + \\ - \sin \phi [1 + \exp(2i\omega L) - 2 \exp i\omega L (1 + \sin \theta \sin \phi)] \}. \quad (49)$$

This equation gives exactly the total response function (150) in [10], where the computation has been realized in the TT gauge.

Eq. (49) is also in perfect agreement with the low frequencies response function in [12].

$$H_{tot}(\omega \rightarrow 0) = -\sin^2 \theta \cos 2\phi. \quad (50)$$

### 3 The signal to noise ratio in the LIGO-LIGO cross-correlation for the detection of relic scalar waves

By considering a stochastic background of relic SGWs, the complex Fourier amplitude  $\tilde{\Phi}$  is treated as a random variable with zero mean value in a way similar to in the Fourier domain [12]. By assuming that the relic SGWs are isotropic and stationary, the ensemble average of the product of two Fourier amplitudes can be written as [12]

$$\langle \tilde{\Phi}^*(f, \hat{\Omega}) \tilde{\Phi}(f', \hat{\Omega}') \rangle = \delta(f - f') \delta^2(\hat{\Omega}, \hat{\Omega}') \tilde{S}_\Phi(f), \quad (51)$$

where  $\hat{\Omega}$  is a unit vector specifying the propagation direction, and by using the explicit definition of the spectrum (1) [12]

$$\tilde{S}_\Phi(f) = \frac{3H_0^2 \Omega_{sgw}(f)}{8\pi^3 f^3}. \quad (52)$$

The quantity

$$\delta^2(\hat{\Omega}, \hat{\Omega}') \equiv \delta(\phi - \phi') \delta(\cos \theta - \cos \theta') \quad (53)$$

is the covariant Dirac delta function on the two-sphere, see [23].

The optimal strategy for a potential detection of a stochastic background of relic SGWs requires the cross-correlation of at least two detectors with uncorrelated noises  $n_i(t)$ ,  $i = 1, 2$  [12]. By following [12], given the two outputs over a total observation time  $T$ ,

$$s_i(t) = S_\Phi^i(t) + n_i(t), \quad (54)$$

a *signal*  $S$  can be constructed:

$$S = \int_{-T/2}^{T/2} s_1(t) s_2(t') Q(t - t'), \quad (55)$$

where  $Q$  is a suitable filter function, usually chosen to optimize the signal to noise ratio (SNR) [12]

$$SNR = \langle S \rangle / \Delta S. \quad (56)$$

In the above equation  $\Delta S$  is the variance of  $S$ .  $Q(t - t')$  is a sharply peaked function about values where  $t - t'$  is comparable to the wave travel time between the two detectors (so that unphysical correlations are ignored) [19]. Hence, by assuming that the observation time is longer than the light travel time between detectors, we get

$$\langle S \rangle = \frac{H_0^2}{5\pi^2} T * Re \left\{ \int_0^\infty df \frac{\tilde{Q}(f) \Omega_{sgw}(f) \gamma(f)}{f^3} \right\}, \quad (57)$$

in the frequency domain, where  $\gamma(f)$  is the so - called overlap reduction function defined in [17] and adapted to scalar waves in [12].

For the computation of the variance, one assumes that, in each detector, the noise is much greater than the strain due to SGWs, obtaining [12]

$$\Delta S^2 \simeq \frac{T}{2} \int_0^\infty df P_1(|f|) P_2(|f|) |\tilde{Q}(f)|^2, \quad (58)$$

where  $P_i(|f|)$  is the one-sided power spectral density of the  $i$  detector [12].

By introducing the inner product [12]

$$(a, b) \equiv Re \left\{ \int_0^\infty df a(f) b(f) P_1(f) P_2(f) \right\}, \quad (59)$$

the squared SNR can be rewritten as

$$(SNR)^2 = 2T \left( \frac{H_0^2}{5\pi^2} \right)^2 \frac{(\tilde{Q}, \frac{\theta(f) \tilde{Q}(f) \Omega_{sgw}(f) \gamma(f)}{f^3 P_1(|f|) P_2(|f|)})}{(\tilde{Q}, \tilde{Q})}, \quad (60)$$

where the Heaviside step function  $\theta(f)$  is introduced in order to insure that the limits of integration are always over positive frequencies [19]. The above ratio is maximal for [12]

$$\tilde{Q} = k \frac{\theta(f) \Omega_{sgw}(f) \gamma(f)}{f^3 P_1(|f|) P_2(|f|)}, \quad (61)$$

where  $k$  is a (real) overall normalization constant [23]. With this optimal choice the signal to noise ratio becomes

$$(SNR) = \sqrt{2T} \frac{H_0^2}{5\pi^2} \sqrt{\int_0^\infty df \frac{\Omega_{sgw}^2(f) \gamma^2(f)}{f^6 P_1(|f|) P_2(|f|)}}. \quad (62)$$

## 4 The generalized overlap reduction function for the advanced LIGO-LIGO cross-correlation

The overlap reduction function for SGWs is given by [12]

$$\gamma(f) = \frac{15}{4\pi} \int d\hat{\Omega} \exp(2\pi i f \hat{\Omega} \cdot \vec{r}_{12}) H_1(f) H_2(f), \quad (63)$$

where  $\vec{r}_{12}$  is the distance between the two detectors and  $H_i(f)$  the angular pattern of the  $i$  detector ( $i = 1, 2$ ). In the literature, the low-frequency approximated angular pattern (50) has been used in the computation of the overlap reduction functions for stochastic backgrounds of relic SGWs, see [12] and references within. Actually, the analysis can be improved with the aid of the frequency dependent angular pattern (49). By putting the origin of the coordinate system in the LIGO site in Hanford we write ( $\omega = 2\pi f$ )

$$\begin{aligned} \gamma(f) = & \frac{15}{4\pi} \int \sin \theta d\theta d\phi \exp(2\pi i f X) \frac{\sin \theta}{4\pi i f L} \{ \cos \phi [1 + \exp(4\pi i f L) - 2 \exp 2\pi i f L (1 + \sin \theta \cos \phi)] + \\ & - \sin \phi [1 + \exp(4\pi i f L) - 2 \exp 2\pi i f L (1 + \sin \theta \sin \phi)] \} \cdot \\ & \frac{\sin(\theta - \theta_1)}{4\pi i f L} \{ \cos(\phi - \phi_1) [1 + \exp(4\pi i f L) - 2 \exp 2\pi i f L (1 + \sin(\theta - \theta_1) \cos(\phi - \phi_1))] + \\ & - \sin(\phi - \phi_1) [1 + \exp(4\pi i f L) - 2 \exp 2\pi i f L (1 + \sin(\theta - \theta_1) \sin(\phi - \phi_1))] \}, \end{aligned} \quad (64)$$

where  $\theta_1 = -28.64^\circ$ ,  $\phi_1 = 71.2^\circ$ ,  $L = 4Km$  and

$$\begin{aligned} X \equiv & d \{ \cos(\phi_1 - \phi) (-\sin \theta_1 + \cos \theta_1 (\cos \phi_1 + \sin \phi_1)) \cdot \\ & (-\sin \theta + \cos \theta (\cos \phi + \sin \phi)) + (\cos \theta_1 + \sin \theta_1 (\cos \phi_1 + \sin \phi_1)) \cdot \\ & (\cos \theta + \sin \theta (\cos \phi + \sin \phi)) - \sin(\phi_1 + \phi) \} \end{aligned} \quad (65)$$

with  $d = 2997.9Km$ . The position and orientation of the two LIGO sites are well known [1].

Eq. (64) is the overlap reduction function for an isotropic stochastic background [19]. It is a dimensionless function of frequency  $f$  which depends entirely on the relative positions and orientations of a pair of detectors [20] and which is angle averaged over all directions [19]. Further details on the overlap reduction function can be find in [20].

The computation of the frequency-dependent overlap reduction function (64) has to be considered together with the one in [9]. In such a work we studied the cross correlation between the Virgo interferometer and the MiniGRAIL resonant sphere for the detection of relic scalar gravitational waves (SGWs). It was shown that the overlap reduction function for the cross correlation between Virgo and the monopole mode of MiniGRAIL is very small, but a maximum was also found in the correlation at about  $2710Hz$ , in the range of the MiniGRAIL sensitivity.

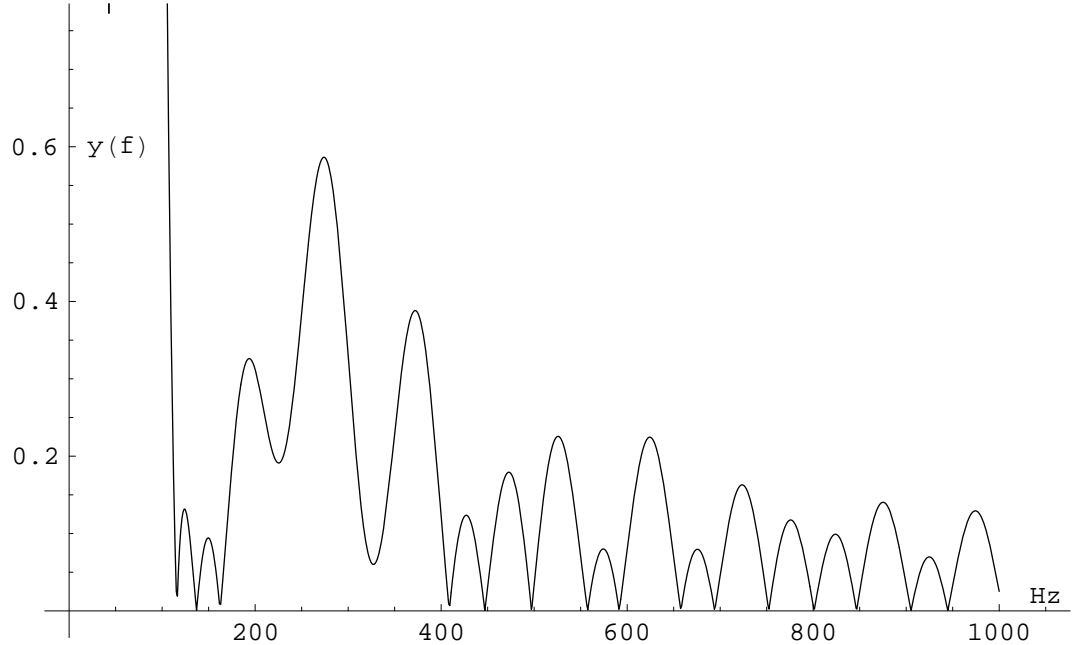


Figure 2: The absolute value of the overlap reduction function (64) in the frequency-range  $10\text{Hz} \leq f \leq 1\text{KHz}$ .

In figure 2, the absolute value of the overlap reduction function (64) is drawn in the frequency-range of Earth based interferometers that is the interval (4). We emphasize that old overlap reduction functions, constructed with the approximated angular pattern (50), guarantee only the coverage of the shorter interval (5). The new overlap reduction function of equation (64) guarantees also the coverage of the high frequency portion  $100\text{Hz} \leq f \leq 1\text{KHz}$ . This is very important for the potential detection of relic SGW at high frequencies.

In figure 2 the value of the overlap reduction function of the two LIGO interferometers for SGWs appears low, thus, in principle, we need a long integration time in order to improve the SNR. A lower bound for the integration time of a potential detection will be released in next Section. This lower bound for the integration time corresponds to an upper bound for the specific SNR of the cross-correlation between the two advanced LIGO.

## 5 The specific signal to noise ratio for scalar waves in a cross-correlation between the two advanced LIGO interferometers

The spectrum of relic GWs is flat in the frequency-range of Earth based interferometers. WMAP observations put strongly severe restrictions on such a spectrum [8, 13, 14]. In fig. 3 we map the spectrum  $\Omega_{sgw}$  choosing the amplitude (determined by the ratio  $\frac{M_{inl}}{M_{Planck}}$  [8, 14] to be *as large as possible, consistent with the WMAP constraints* [8, 13, 14]. The inflationary spectrum rises quickly at low frequencies (waves which re-entered in the Hubble sphere after the Universe became matter dominated) and falls off above the (appropriately redshifted) frequency scale  $f_{max}$  associated with the fastest characteristic time of the phase transition at the end of inflation. The amplitude of the flat region depends on the energy during the inflationary stage [8, 14]. As WMAP data are consistent with a maximum inflationary scale  $M_{inl} = 2 \cdot 10^{16} \text{GeV}$  [8, 13, 14], this means that today, at LIGO and LISA frequencies, indicate by the lines in fig. 3, one obtains the bound of equation (3).

Let us apply the new overlap reduction function obtained in eq. (64). To detect a stochastic background of relic scalar GWs we need to obtain a signal to noise ratio equal, at least, to the one in eq. (62). By inserting  $(SNR) = 1$  in eq. (62) and solving in respect to the observation time one gets

$$T = \left(\frac{5\pi^2}{H_0^2}\right)^2 \frac{1}{2 \int_0^\infty df \frac{\Omega_{sgw}^2(f) \gamma^2(f)}{f^6 P_1(|f|) P_2(|f|)}}. \quad (66)$$

Let us insert in eq. (66) the value of eq. (64) of the new overlap reduction function and the value of the spectrum in eq. (3). For both of  $P_1(|f|)$  and  $P_2(|f|)$  we use the analytical fit of [12] for the noise spectral density of advanced LIGO, which is

$$P(f) = \frac{P_0}{5} \left[ \left(\frac{f_0}{f}\right)^4 + 2 + 2\left(\frac{f}{f_0}\right)^2 \right] \quad (67)$$

where  $P_0 = 2.3 \cdot 10^{-48} \text{Hz}^{-1}$  and  $f_0 = 75 \text{Hz}$ .

In this way, by integrating the right hand side of eq. (66) in all the range of eq. (4), which is the total frequency range of Earth based interferometers, one obtains

$$T \sim 8 \cdot 10^5 \text{years}. \quad (68)$$

The assumption that all the scalar perturbation in the Universe are due to a stochastic background of relic SGWs is quit strong, but the result can be considered like a lower bound for the observation time.

To better understand the difference between the response function of this paper and previous low-frequency approximated ones a brief comparison is now discussed. In the previous literature, people inserted the approximated response

function of eq. (50) in eq. (66). More, the integration was performed only in the low frequencies range of eq. (5) where the low frequencies approximation of eq. (50) is correct. If one inserts the old, approximated, overlap reduction function in eq. (66) and uses the same eq. (67) for both of  $P_1(|f|)$  and  $P_2(|f|)$  and the same value of the spectrum in eq. (3), the observation time obtained from eq. (66) results overpriced

$$T \sim 7 * 10^6 \text{ years.} \quad (69)$$

An order of magnitude is gained by introducing the new overlap reduction function and by integrating in all the frequency range of Earth based interferometers that is the interval of eq. (4).

The times involved in the two results (the correct one and the overpriced one) are substantially longer than the entire existence of the human species [19]. In order to be interesting, one has to determine the necessary sensitivity to bring the observation time down to a reasonable value (e.g. the lifetime of a graduate student) [19]. For this goal, one notes from eq. (62) that a gain in sensitivity higher than 2 orders of magnitude, which will permit to reduce of 5 orders of magnitude the noise spectral density of interferometric GW detectors, could in principle provide  $(SNR) = 1$  for observation times which are not too long (order of some years). In this case, the order of magnitude gained with the new overlap reduction function will be very important for the signal detection. This sensitivity looks to be not beyond the scope of any known technology. In fact, a fundamental obstacle which limited the sensitivity of interferometric GW detectors was the vacuum (zero-point) fluctuations of the electromagnetic field. Recently, it has been shown that a quantum technology—the injection of squeezed light—offers a solution to this problem [21]. On the other hand, the third generation of GW detectors will limit the effect of the seismic noise, and, through cryogenic facilities, will cool down the mirrors to directly reduce the thermal vibration of the test masses [22]. By using eq. (67) one gets  $P(100 \text{ Hz}) \sim 10^{-47} \text{ Hz}^{-1}$  which gives a sensitivity in strain of  $h \sim 10^{-25}$  at 100 Hz, i.e. the frequency where the sensitivity of interferometric GW detectors is highest. The Einstein Telescope will be sensitive to intrinsic GW amplitudes of order  $h \sim 10^{-27}$  in the frequency range 6 Hz to 3 kHz [22]. Therefore, a gain in sensitivity higher than 2 orders of magnitude looks a concrete possibility.

## 6 Conclusions

In earlier work we studied the cross correlation between the Virgo interferometer and the MiniGRAIL resonant sphere for the detection of relic SGWs. It was shown that the overlap reduction function for the cross correlation between Virgo and the monopole mode of MiniGRAIL is very small, but a maximum was also found in the correlation at about 2710 Hz, in the range of the MiniGRAIL sensitivity.

In this paper the analysis has been improved. After carefully reviewing the response function of interferometers to SGWs directly in the gauge of the

local observer, the result has been used to analyze the cross-correlation between the two LIGO interferometers in their advanced configuration for a potential detection of relic SGWs and to release a lower bound for the integration time of such a detection. By using a new, frequency-dependent, overlap reduction function, a comparison with previous low-frequency approximations has been performed too. This is the first time that such a cross-correlation is computed in all the frequency spectrum of relic SGWs. The computation of a better signal to noise ratio is very important to understand if a scalar component of GWs is present at high frequency.

With the new overlap reduction function, an order of magnitude is gained concerning the integration time for detecting relic SGWs signal, and this could be very important for a potential detection if advanced projects further improve their sensitivity.

## 7 Acknowledgements

The R. M. Santilli Foundation has to be thanked for partially supporting this paper (Research Grant Number RMS-TH-5735A2310). I thank an unknown referee for useful comments.

## Riferimenti bibliografici

- [1] The LIGO Scientific Collaboration, *Class. Quant. Grav.* 26, 114013 (2009).
- [2] C. Corda, *Op. Astr. Journ.* 4, (Suppl 1-M5) 75-83 (2011).
- [3] Y. Zhang, M.L. Tong and Z.W. Fu, *Phys. Rev. D* 81, 101501 (2010).
- [4] I. Agullo, J. Navarro-Salas, G. J. Olmo and L. Parker, arXiv:1002.3914, to appear in the Proceedings of Spanish Relativity Meeting 2009 (ERE 09), Bilbao (Spain).
- [5] M. L. Tong and Y. Zang, *Phys. Rev. D* 80, 084022 (2009).
- [6] W. T. Ni, *Int. J. Mod. Phys. D* 18, 2195-2199 (2009).
- [7] T.Y. Xia and Y. Zhang, *Phys. Rev. D* 79, 083002 (2009).
- [8] S. Capozziello, C. Corda and M. F. De Laurentis, *Mod. Phys. Lett. A* 22, 35, 2647-2655 (2007).
- [9] C. Corda, *Mod. Phys. Lett. A* 22, 1727-1735 (2007).
- [10] S. Capozziello and C. Corda, *Int. J. Mod. Phys. D* 15, 1119-1150 (2006).
- [11] M. E. Tobar , T. Suzuki and K. Kuroda, *Phys. Rev. D* 59 102002 (1999).
- [12] M. Gasperini and C. Ungarelli, *Phys. Rev. D* 64, 064009 (2001).

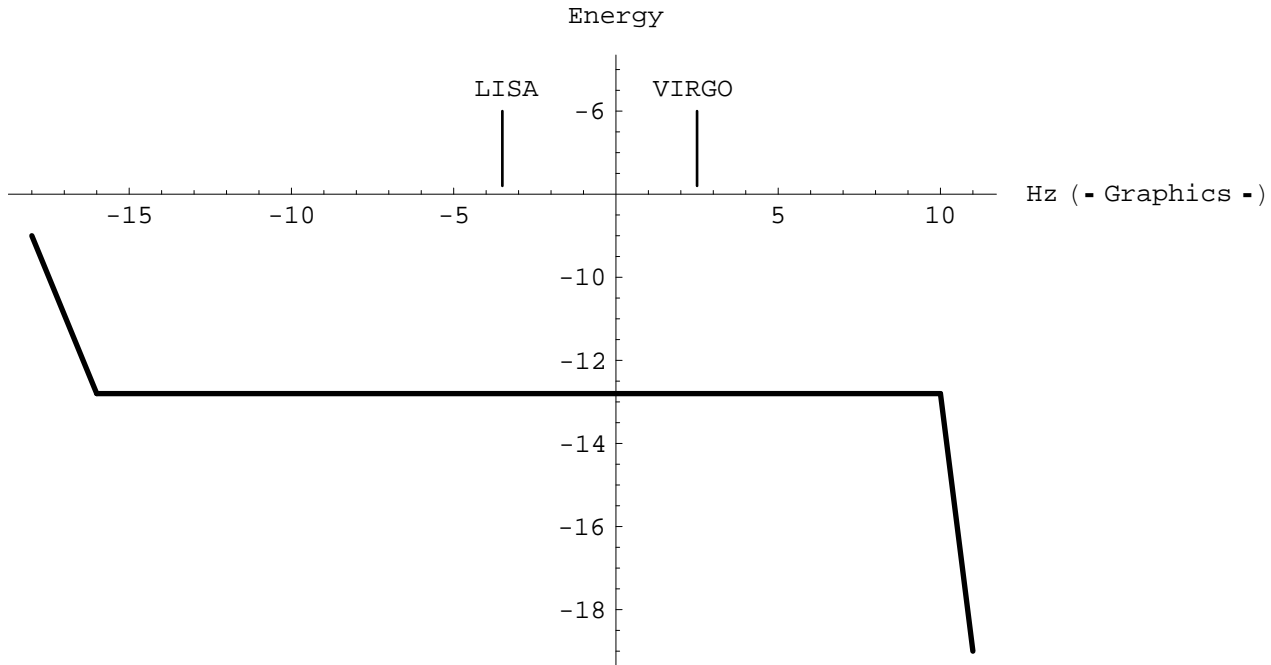


Figure 3: The spectrum of relic SGWs in inflationary models is flat over a wide range of frequencies. The horizontal axis is  $\log_{10}$  of frequency, in Hz. The vertical axis is  $\log_{10} \Omega_{gsw}$ . The inflationary spectrum rises quickly at low frequencies (waves which re-entered in the Hubble sphere after the Universe became matter dominated) and falls off above the (appropriately redshifted) frequency scale  $f_{max}$  associated with the fastest characteristic time of the phase transition at the end of inflation. The amplitude of the flat region depends on the energy during the inflationary stage; we have chosen the largest amplitude consistent with the WMAP constraints on scalar perturbations. This means that at LIGO and LISA frequencies,  $\Omega_{sgw}(f)h_{100}^2 < 9 * 10^{-13}$ . Adapted from ref. [8]

- [13] C. L. Bennet et al., *Astrophys. J. Suppl.* 148, 1 (2003).
- [14] Abbot et al. *Nature* 460, 990-994 (2009).
- [15] C. Brans and R. H. Dicke, *Phys. Rev.* 124, 925 (1961).
- [16] C. W. Misner, K. S. Thorne and J. A. Wheeler, *Gravitation*, W.H.Feeman and Company (1973).
- [17] E. Flanagan, *Phys. Rev. D* 48, 2389 (1993).
- [18] C. Corda, *Int. J. Mod. Phys. D* 18, 2275-2282 (2009).
- [19] Private communication with an unknown referee.
- [20] B. Allen, Proceedings of the Les Houches School on Astrophysical Sources of Gravitational Waves, eds. Jean-Alain Marck and Jean-Pierre Lasota Cambridge, pp. 373-417 (Cambridge University Press, Cambridge, England 1998).
- [21] The LIGO Scientific Collaboration, *Nat. Phys.* online (2011), doi:10.1038/nphys2083.
- [22] B. Sathyaprakash et al., Proceedings of the Moriond Meeting 2011 at La Thuille, Italy (2011), pre-print in arXiv:1108.1423.
- [23] B. Allen and J. D. Romano, *Phys. Rev. D* 59, 102001 (1999).